Supplementary Figure 1.

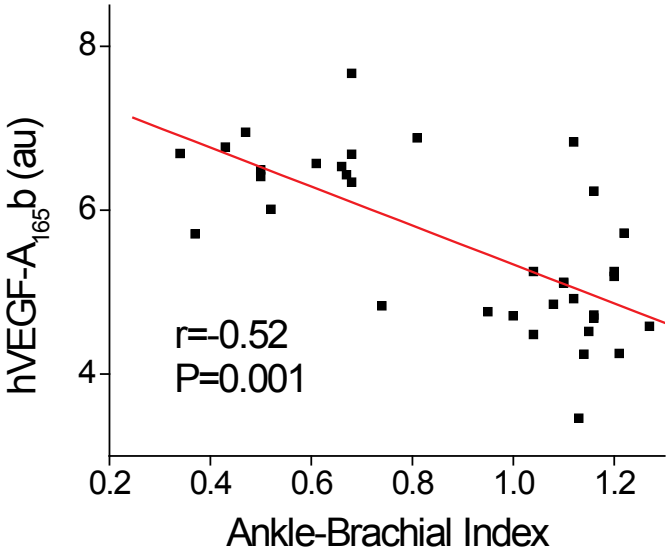

Supplementary Figure 1. Relation of hVEGF-A_{165}b with PAD severity in humans. Higher serum levels of inhibitory hVEGF-A_{165}b were associated with lower ABI, a measure of atherosclerotic obstructive disease in the lower extremity (*n* = 35) Spearman correlation analysis.

Supplementary Figure 2.

a

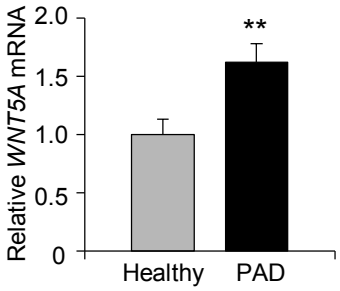

b

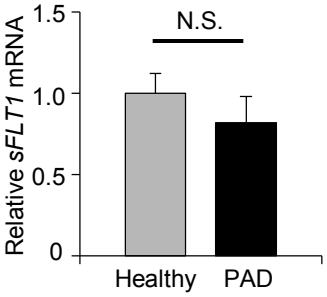

c

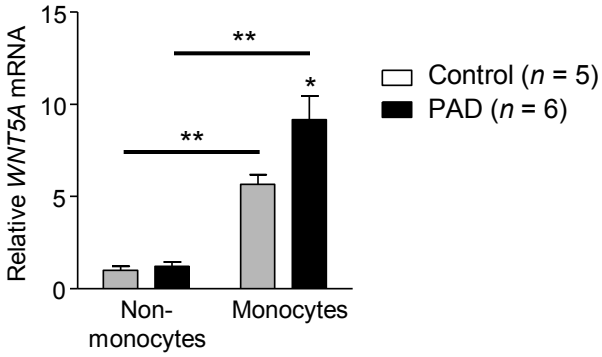

Supplementary Figure 2. Expression of *WNT5A* and *sFLT1* in clinical PAD. **a,** *WNT5A* mRNA expression was measured by qRT-PCR using peripheral blood mononuclear cells from PAD (n = 25) and healthy (n = 25) subjects. Results are shown as the mean ± S.E. **b,** *sFLT1* mRNA expression was measured by qRT-PCR using peripheral blood mononuclear cells in PAD (n = 25) and healthy (n = 25) subjects. **c,** *WNT5A* mRNA expression was measured in monocytes and non-monocytes (CD3, CD7, CD16, CD19, CD56, CD123 and glycophorin A magnetic separation) of control (n = 5) and PAD patients (n = 6). Analyses by t-test by independent or paired-sample t-test as appropriate. *P < 0.05, **P < 0.01.

Supplementary Figure 3.

a

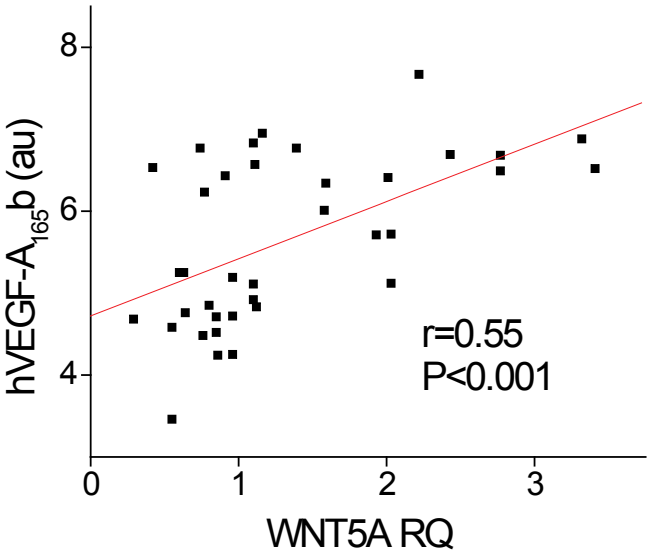

b

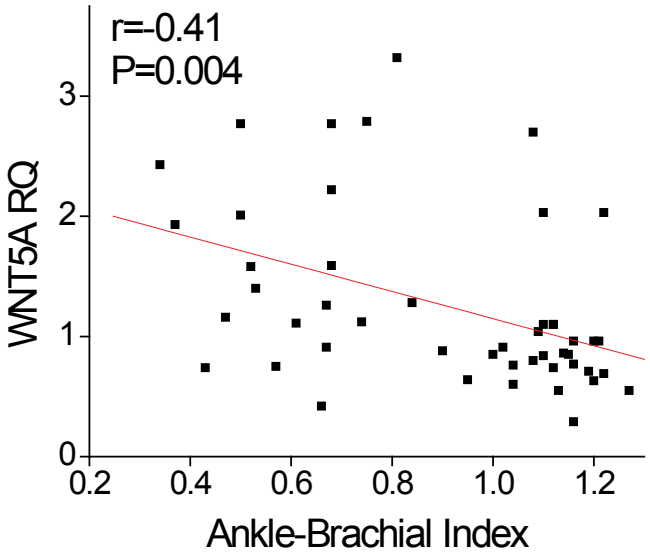

Supplementary Figure 3. Expression of *WNT5A* in human PAD. A. In patients, higher *WNT5A* expression in PBMCs was associated with higher circulating inhibitory hVEGF-A_{165}b (*n* = 37). B. In patients, higher *WNT5A* expression in PBMCs was associated with lower ABI (*n* = 49) Analyses by Spearman correlation.

Supplementary Figure 4.

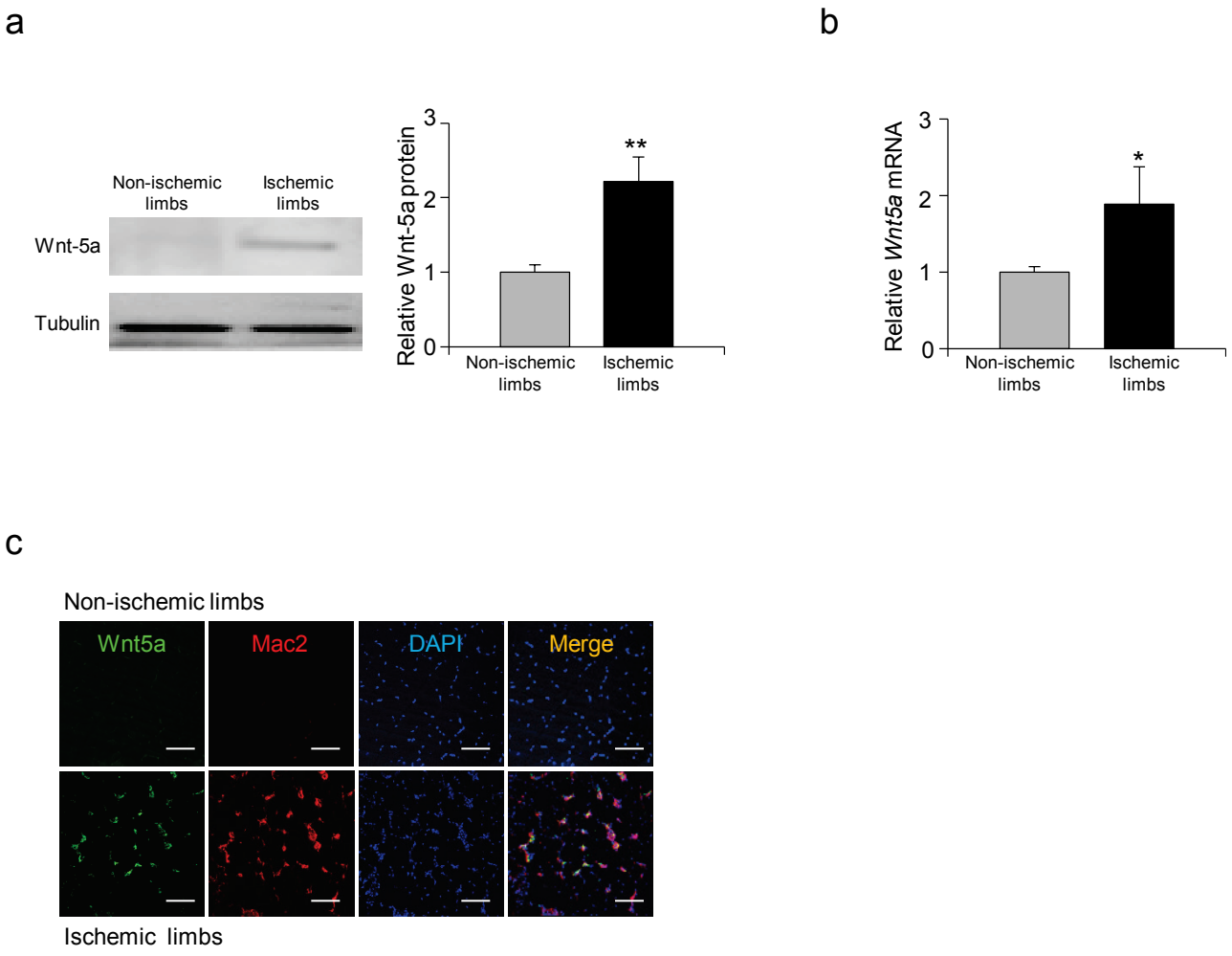

Supplementary Figure 4. Increased expression of Wnt5a in the ischemic limbs of wild-type mice. a, Wnt5a levels were determined by western blot analysis in the non-ischemic (gray bar) and ischemic (black bar) gastrocnemius muscle at 3 days after surgery in C57BL/6 mice. Representative blots from three independent experiments are shown. Relative Wnt5a protein was quantified using ImageJ. Immunoblots were normalized to tubulin signal. Results are shown as the mean ± S.E. (n = 5/group). $^{**}P < 0.01$ (Student's t-test). **b**, *Wnt5a* mRNA expression was measured by qRT-PCR in the non-ischemic (gray bar) and ischemic (black bar) muscle at 3 days after surgery of C57BL/6 mice. Results are shown as the mean ± S.E. (n = 5/group). $^{*}P < 0.05$ (Student's t-test). **c**, Representative images of immunostaining for Wnt-5a (green) and Mac2 (red) in the non- (top panel) or ischemic (bottom panel) from C57BL/6 mice. Scale bars are 100 μm.

Supplementary Figure 5.

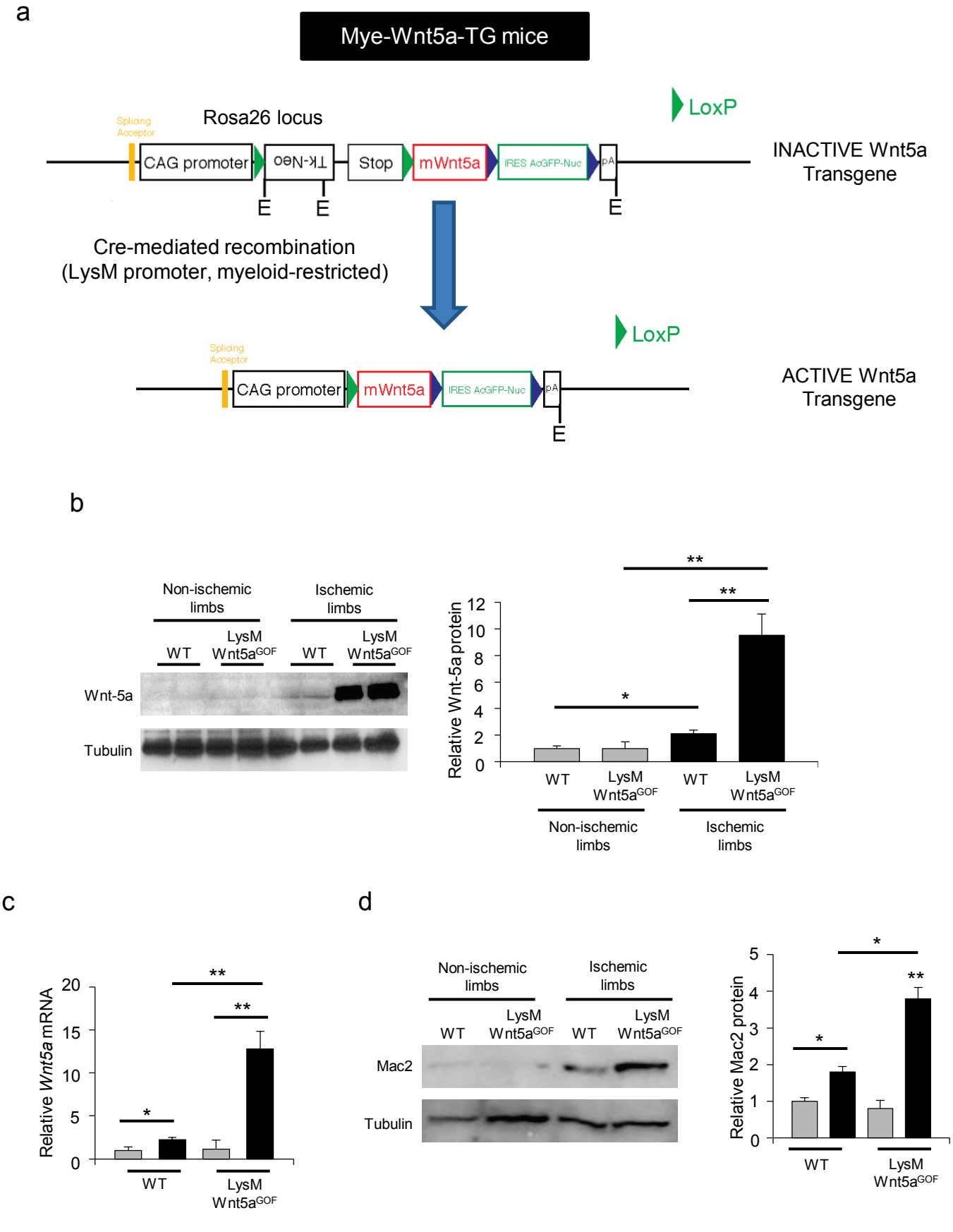

Supplementary Figure 5. Macrophage derived Wnt5a was increased in the ischemic limbs of macrophage specific Wnt5a gain of function mice. a, Mice exhibiting Wnt5a overexpression restricted to myeloid cells were generated by a Cre/LoxP strategy. A Cre-inducible Wnt5a transgene is inserted into the Rosa26 locus of C57Bl/6 mice. These mice were interbred with LysozymeM-Cre (LysM-Cre) mice (Jackson Laboratories) to induce Wnt5a overexpression specifically in myeloid cells. **b**, Wnt-5a protein levels was determined by western blot analysis in the non-ischemic (gray bar) and ischemic (black bar) gastrocnemius muscle at 3 days after surgery in wild-type or LysM-Wnt5a^{GOF} mice. Relative Wnt-5a protein level was quantified using ImageJ. Immunoblots were normalized to tubulin signal. Results are shown as the mean ± S.E. (n = 5/group). ANOVA and post-hoc by Dunnett test. **c**, *Wnt5a* mRNA expression was measured by qRT-PCR in the non-ischemic (gray bar) and ischemic (black bar) muscle at 3 days after surgery of wild-type or LysM-Wnt5a^{GOF} mice. Results are shown as the mean ± S.E. (n = 5/group). ANOVA and post-hoc by Dunnett test. **d**, Mac2 protein levels was determined by western blot analysis in the non-ischemic (gray bar) and ischemic (black bar) gastrocnemius muscle at 3 days after surgery in wild-type or LysM-Wnt5a^{GOF} mice. Relative Mac2 protein was quantified using ImageJ. Immunoblots were normalized to tubulin signal. Results are shown as the mean ± S.E. (n = 5). ANOVA and post-hoc by Dunnett test. *P < 0.05, **P < 0.01.

Supplementary Figure 6.

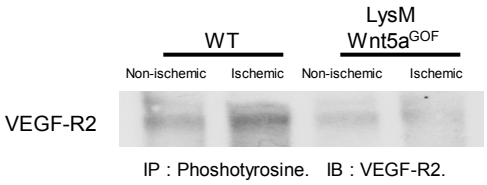

Supplementary Figure 6. Impaired tyrosine phosphorylation of VEGFR2 in the ischemic limbs of LysM-Wnt5a^{GOF} mice. Protein (500 μg) was immunoprecipitated (IP) from non-ischemic and ischemic gastrocnemius muscle lysate of WT and LysMWnt5a^{GOF} mice using mouse anti-phosphotyrosine antibody. An immunoblot (IB) was then performed with mouse anti-VEGFR2 antibody.

Supplementary Figure 7.

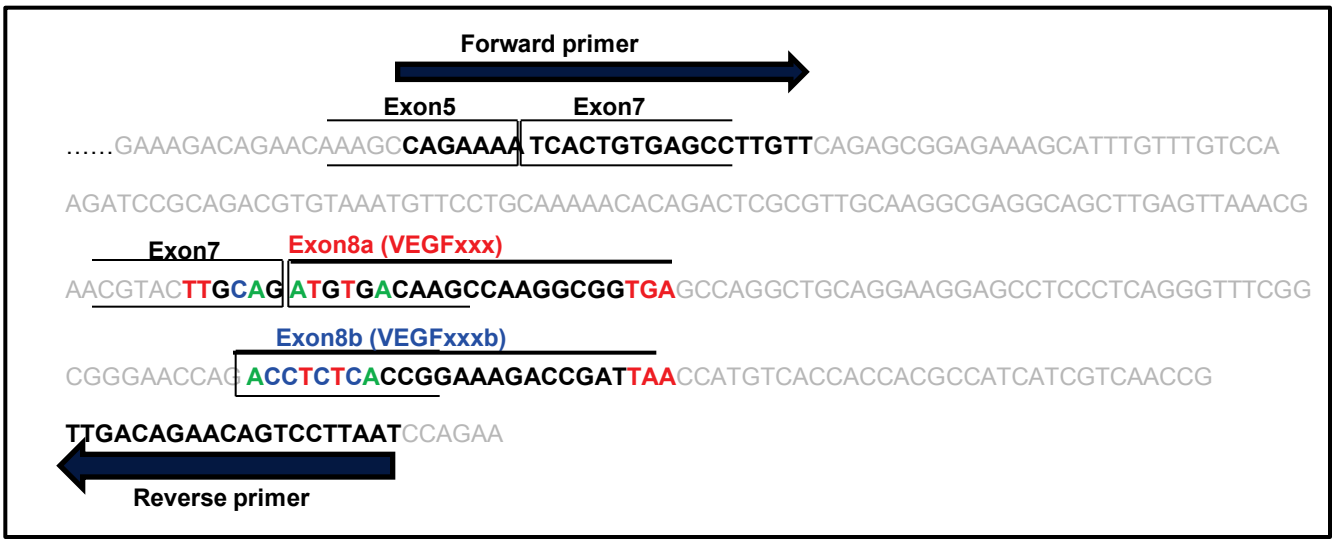

Supplementary Figure 7. Strategy for the identification of mouse VEGF-A_{165}b. **C**onventional PCR primers were designed to amplify both m*Vegfa*$_{164}$*a* and m*Vegfa*$_{165}$*b*. The forward primer is specific for the exon 5/7 boundary for mouse *Vegfa*$_{164}$*a* and *Vegfa*$_{165}$*b*, and the reverse primer is located in the 3'-UTR of the mouse *Vegfa* gene. The m*Vegfa*$_{164}$*a* isoform, containing exon8a, was detected as a 281bp PCR product. The m*Vegfa*$_{165}$*b* isoform, containing exon8b, was detected as a 215bp PCR product.

Supplementary Figure 8.

```
Human MNFLLSWVHWSLALLLYLHHAKWSQAAPMAEGGGQNHHEVVKFMDVYQRSYCHPIETLVD
Mouse MNFLLSWVHWTLALLLYLHHAKWSQAAPT T EGE - QKSHEV I KFMDVYQRSYCRPIETLVD
Rat   MNFLLSWVHWTLALLLYLHHAKWSQAAPT T EGE - QKAHEVVKFMDVYQRSYCRPIETLVD

Human IFQEYPDEIEYIFKPSCVPLMRCGGCCNDEGLECVPTEESN I TMQIMRIKPHQGQHIGEM
Mouse IFQEYPDEIEYIFKPSCVPLMRCAGCCNDEALECVPTSESN I TMQIMRIKPHQSQHIGEM
Rat   IFQEYPDEIEYIFKPSCVPLMRCAGCCNDEALECVPTSESNVTMQIMRIKPHQSQHIGEM

Human SFLQHNKCECRPKKDRARQENPCGPCSERRKHLFVQDPQTCKCSCKNTDSRCKARQLELN
Mouse SFLQHSRCECRPKKDRT KPENHCEPCSERRKHLFVQDPQTCKCSCKNTDSRCKARQLELN
Rat   SFLQHSRCECRPKKDRT KPENHCEPCSERRKHLFVQDPQTCKCSCKNTDSRCKARQLELN
```

Exon8b

```
Human ERTCR SLTRK - D
Mouse ERTCR PLTGKT D
Rat   ERTCR PLTGKT D
```

VEGF-Axxxb

	Signal peptide	Mature cleaved polypeptide	Full length amino acid
Human VEGF-A_{165} b	26 aa	165 aa	191 aa
Mouse VEGF-A_{165} b	26 aa	165 aa	191 aa
Rat VEGF-A_{165} b	26 aa	165 aa	191 aa

Exon8a

```
CDKPRR
CDKPRR
CDKPRR
```

VEGF-Axxxa

	Signal peptide	Mature cleaved polypeptide	Full length amino acid
Human VEGF-A_{165}a	26 aa	165 aa	191 aa
Mouse VEGF-A_{164}a	26 aa	164 aa	190 aa
Rat VEGF-A_{164}a	26 aa	164 aa	190 aa

Supplementary Figure 8. Predicted protein sequences of mouse, human and rat VEGF-A_{165}b. Alignment of the predicted protein sequences of human VEGF-A_{165}b, mouse VEGF-A_{165}b and rat VEGF-A_{165}b. Homologous amino acids are shaded in gray.

Supplementary Figure 9.

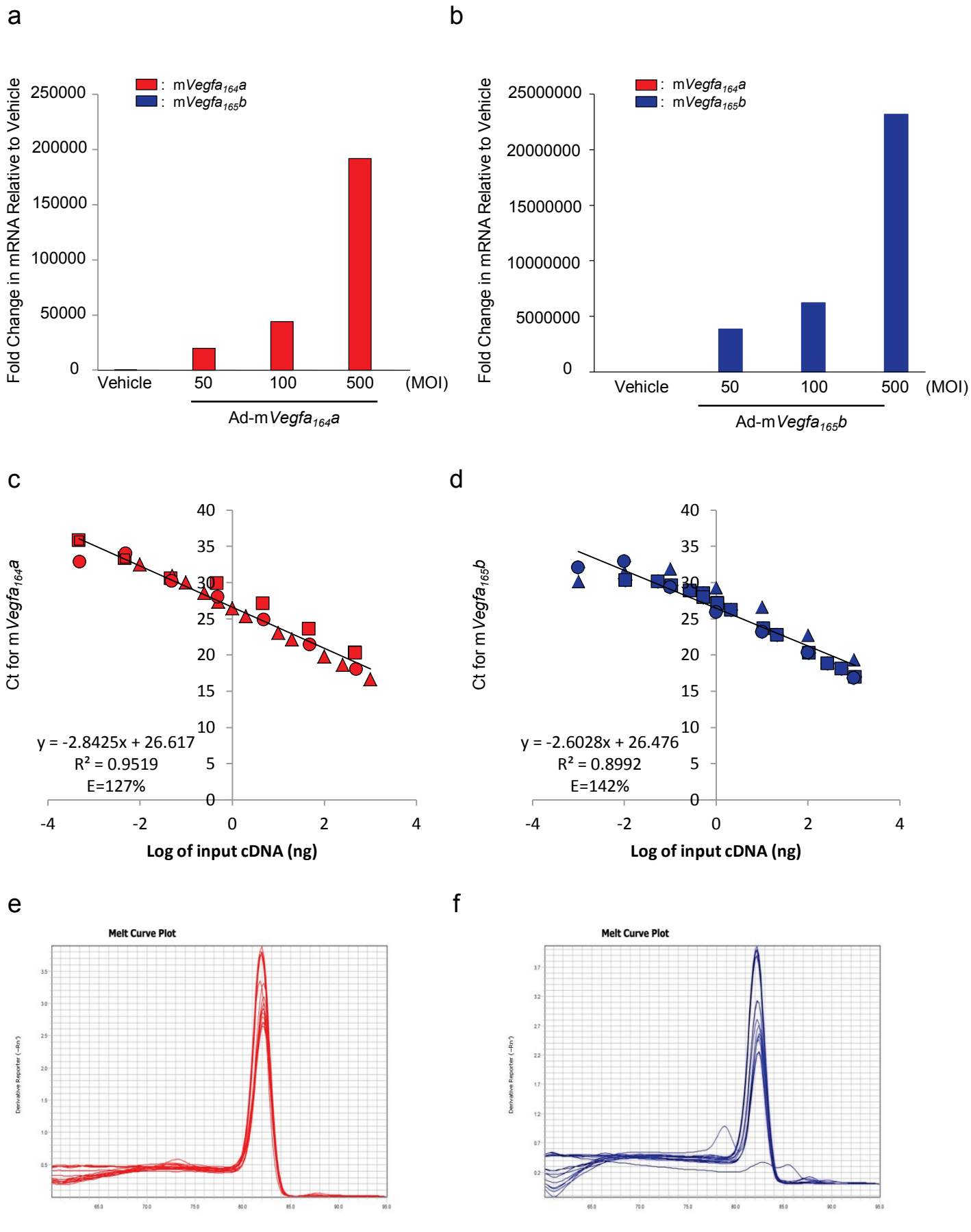

Supplementary Figure 9. Validation of exon specific qPCR primers to detect m*Vegfa*$_{164}$*a* and m*Vegfa*$_{165}$*b*. Specificity and efficiency of the primers were tested by infection of HEK293A cells with adenovirus constructs containing either mVEGF-A$_{164}$a or mVEGF-A$_{165}$b. **a,** Infection of HEK293A cells at indicated multiplicities of infection (MOIs) with adenoviral constructs expressing mouse *Vegfa*$_{164}$*a* resulted in specific detection by the m*Vegfa*$_{164}$*a* primers using the delta-Ct method and normalized to *Gapdh*. The primers for m*Vegfa*$_{165}$*b* failed to recognize overexpressed m*Vegfa*$_{164}$*a*. Data are representative of three independent experiments. **b**, Infection of HEK293A cells at indicated MOIs with adenovirus construct for mouse *Vegfa*$_{165}$*b* was detected by the isoforms specific m*Vegfa*$_{165}$*b* primers, but was not recognized by the m*Vegfa*$_{164}$*a* primers. Data shown are representative of three independent experiments. **c, d,** To determine primer efficiency, samples from the 50 MOI infections were subjected to a seven point, ten-fold dilution series. Following qPCR amplification a standard curve of cut threshold (Ct) versus log of input cDNA concentration was plotted. Primer efficiency (E) was calculated as $E = 10^{(-1/slope)}$ using the slope of the standard curve. Data represent three dilution series from three independent samples, represented by the circle, square and triangle shapes. The standard curves were calculated using all data sets. Both m*Vegfa*$_{164}$*a* and m*Vegfa*$_{165}$*b* demonstrated linearity in the standard curve across six orders of magnitude in the dilution series. **e, f,** Melt curve analysis resulted in a single peak for the product amplified by the m*Vegfa*$_{164}$*a* primers (**e**) and the m*Vegfa*$_{165}$*b* primers (**f**). The melt curves shown are from the experiments described in c and d.

Supplementary Figure 10.

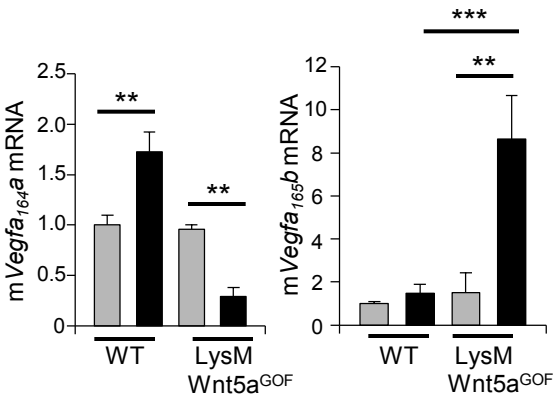

Supplementary Figure 10. Elevated murine $Vegfa_{165}b$ transcript in the ischemic limbs of LysM-Wnt5a^{GOF} mice. Quantitative RT-PCR of m*Vegfa*$_{164}$*a* and m*Vegfa*$_{165}$*b* mRNA expression in the contralateral non-ischemic (gray bar) and ischemic muscle at 7 days after surgery using primer sets that specifically amplify exon 8a- or 8b-containing transcripts. Results are shown as the mean ± S.E. (*n* = 5/group). ANOVA post-hoc Tukey HSD. ***P* < 0.01, ****P* < 0.001

Supplementary Figure 11.

a

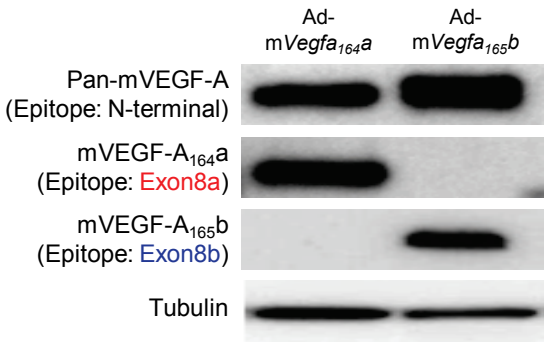

b

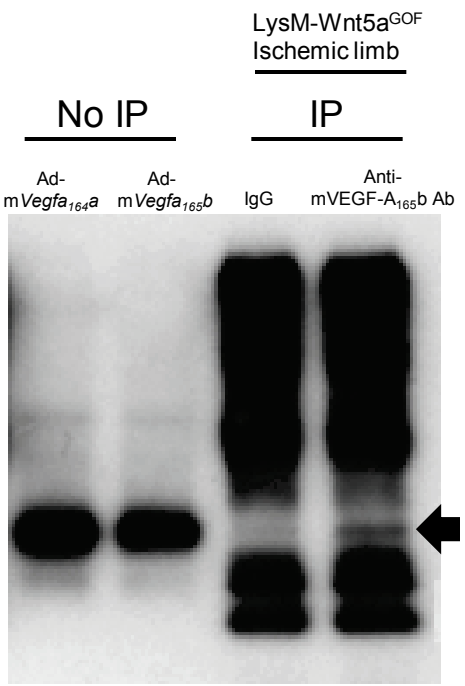

IB : Goat anti – Pan-VEGF-A Ab

Supplementary Figure 11. Specificity of anti-mouse VEGF-A_{165}b antibody. a, Total mVEGF-A, mVEGF-A_{164}a and mVEGF-A_{165}b were measured using specific antibodies in western blot analysis of Ad-m*Vegfa*$_{164}$*a*- or Ad-m*Vegfa*$_{165}$*b*-transfected HUVECs. **b**, Protein (500 μg) was immunoprecipitated (IP) from the ischemic gastrocnemius muscle at 7 days after surgery lysate of LysMWnt5a^{GOF} mice using control rabbit IgG or rabbit anti-mVEGF-A_{165}b antibody. Immunoblot (IB) was then performed with goat anti-pan-VEGF-A antibody. Lysates from VEGF-A_{164}a or mVEGF-A_{165}b transduced HUVECs were used as positive controls for the western blot (left lanes).

Supplementary Figure 12.

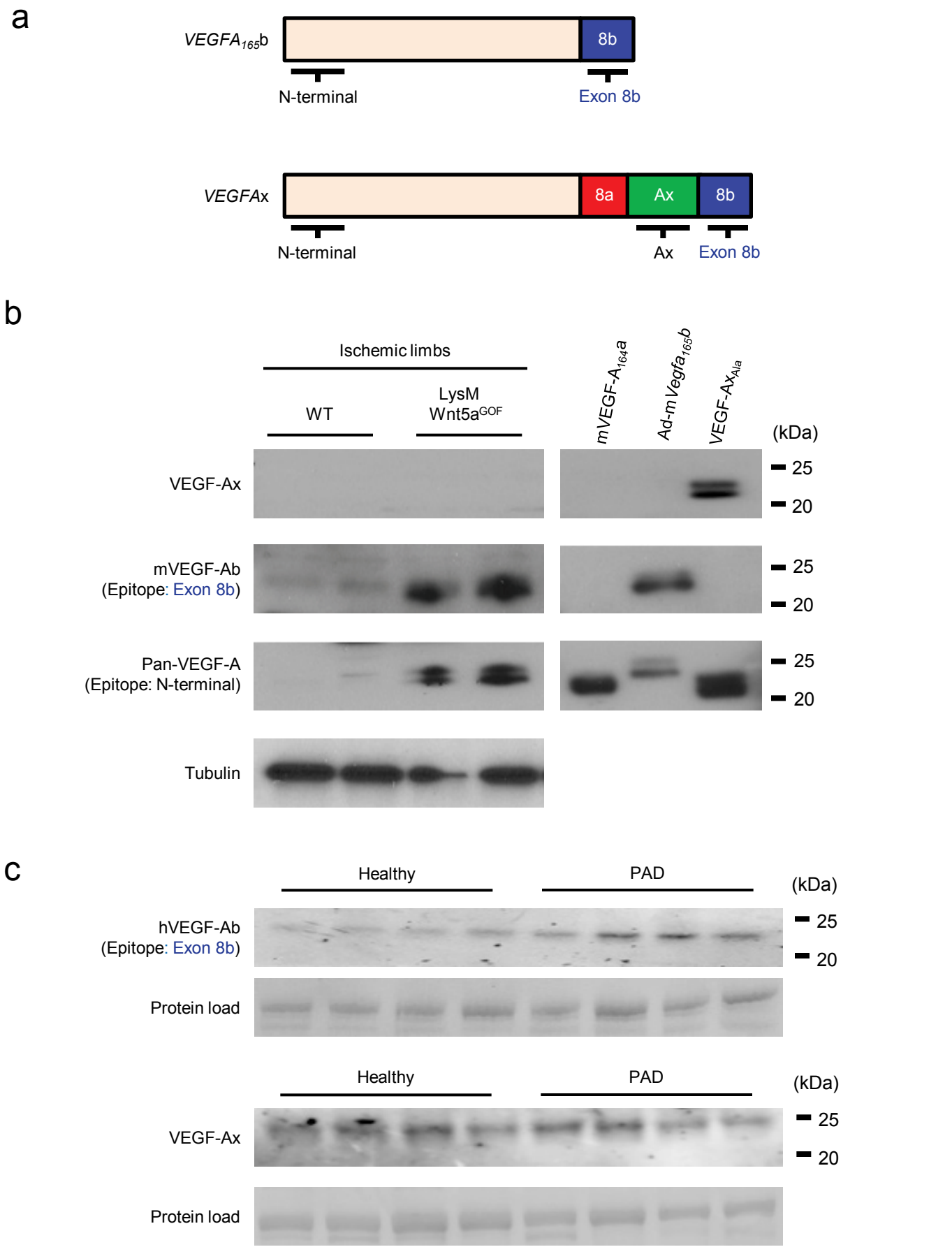

Supplementary Figure 12. Analysis of VEGF-Ax expression in ischemic mouse tissue and in sera from PAD and healthy control subjects. a, A schematic of the exon structure of *VEGFA*$_{165}$*b* (top) and *VEGFAx* (bottom) demonstrating the regions recognized by the N-terminal "pan" VEGF-A, exon 8b and Ax extension region-specific antibodies. **b**, Total VEGF-A, mVEGF-A$_{165}$b and VEGF-Ax protein expression were determined by western blot analysis in the ischemic muscle at 7 days after surgery. **c**, Serum protein expression of hVEGF-A$_{165}$b and VEGF-Ax were measured in PAD (n = 4) and healthy (n = 4) subjects by western blot analysis.

Supplementary Figure 13.

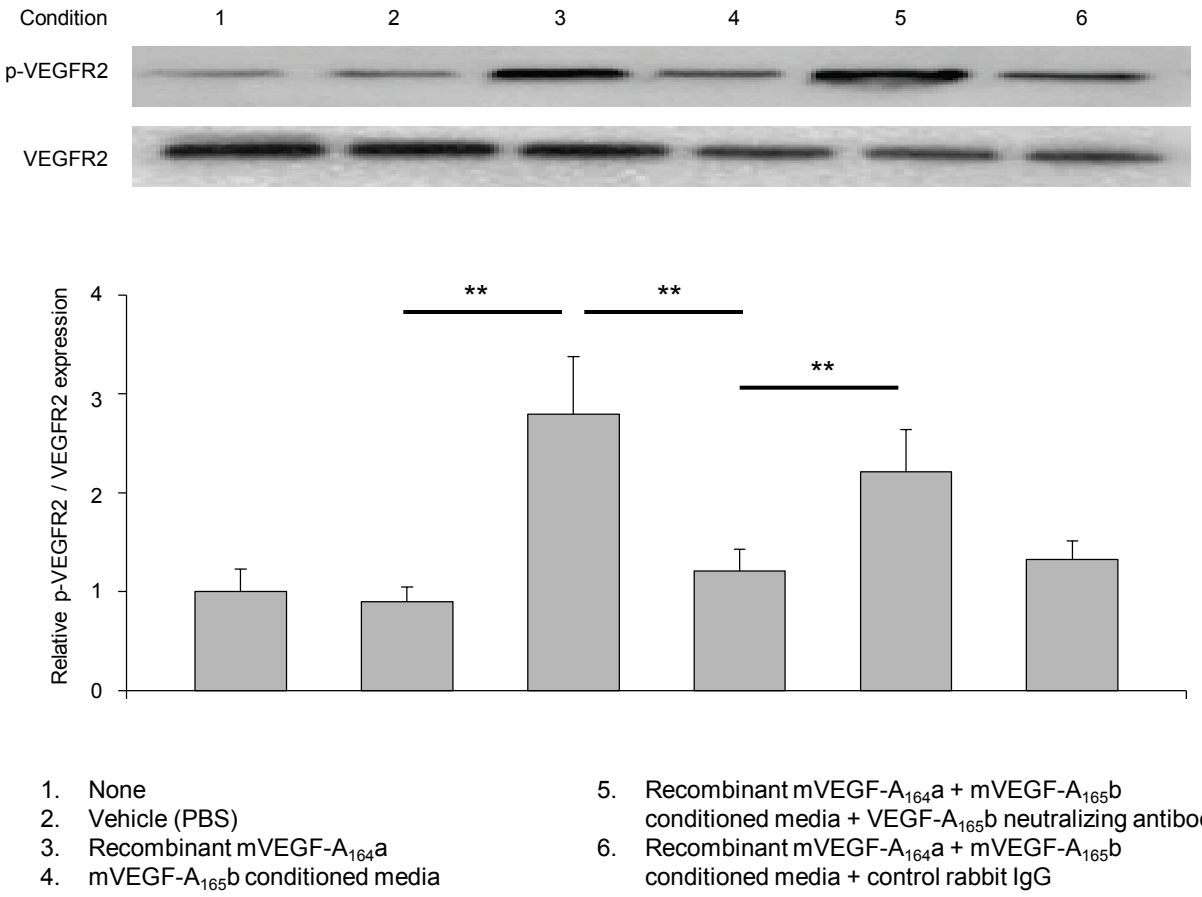

Supplementary Figure 13. Antibody neutralization of VEGF-A_{165}b in vitro. Serum-deprived HUVECs were treated with recombinant mVEGF-A_{164}a in the presence or absence of mVEGF-A_{165}b conditioned media and in the presence or absence of anti-VEGF-A_{165}b neutralizing antibody. HUVECs were transduced with adenoviral vectors expressing mouse *Vegfa$_{165}$b* (Ad-m*Vegfa$_{165}$b*) at 100 MOI for 8 hours followed by 24 hours of incubation in serum-free media to produce the Ad-m*Vegfa$_{165}$b* conditioned media. Serum-deprived HUVECs were pretreated with or without neutralizing antibody for 15 minutes before stimulation with recombinant VEGF-A_{164}a (10 ng/ml) and/or mVEGF-A_{165}b conditioned media for 15 minutes prior to preparation of cell lysates. Lysates were then immunoblotted with antibodies that target phosphorylated VEGFR-2 (951) and total VEGFR-2. The figures are representative of at least three separate experiments with similar results. Results are shown as the mean ± S.E. (*n* = 3/group). ANOVA with post-hoc Tukey HSD test. $^{**}P < 0.01$.

Supplementary Figure 14.

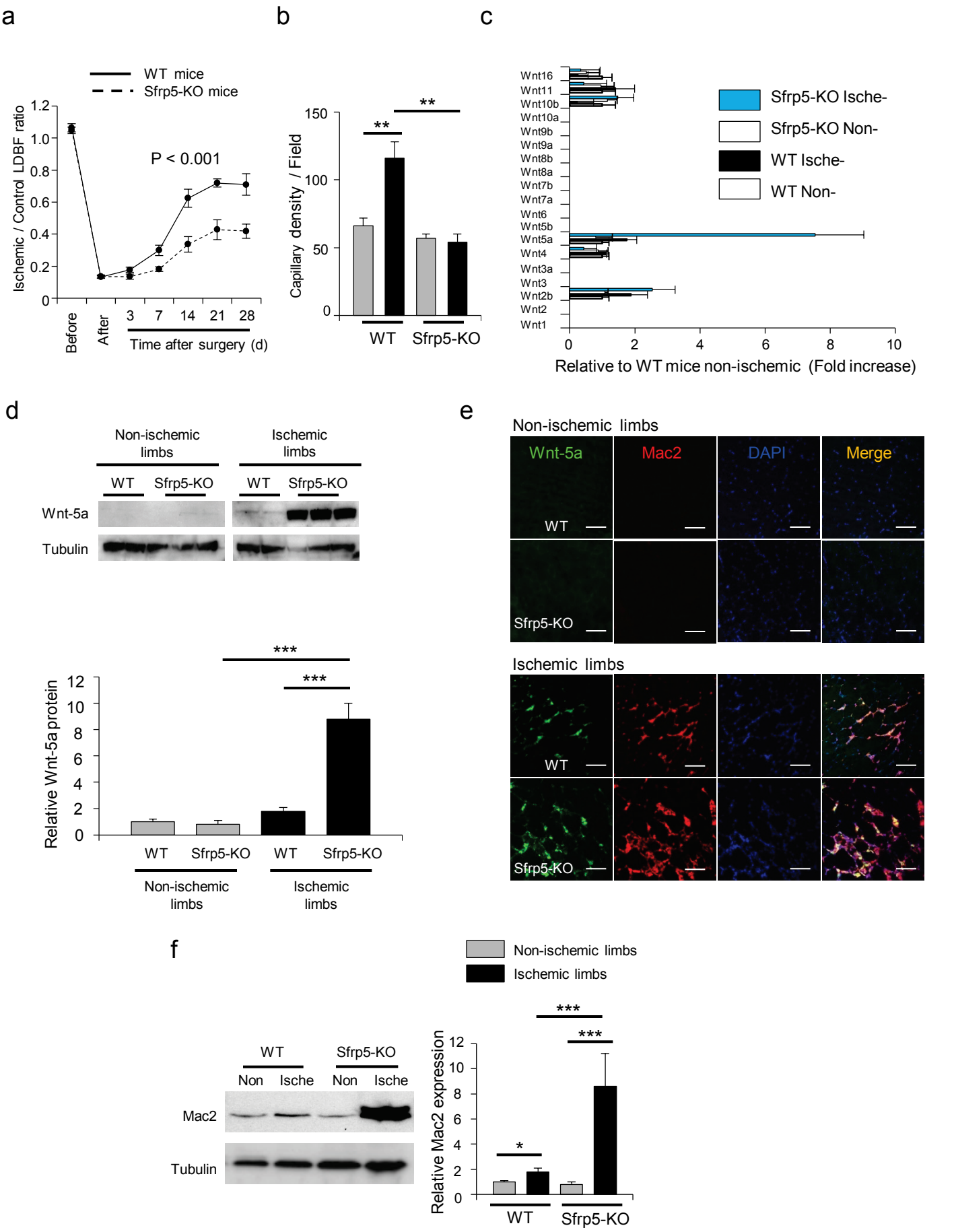

Supplementary Figure 14.

g

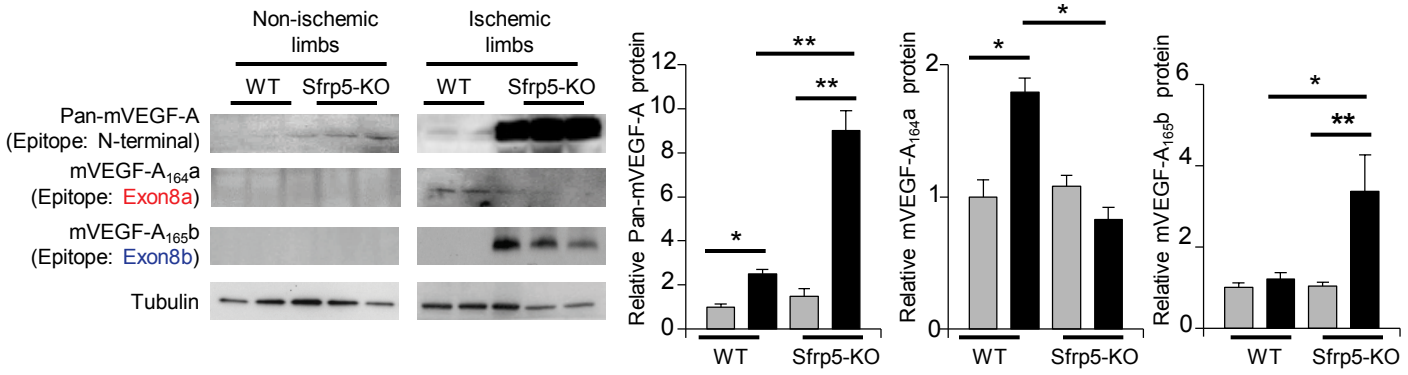

h

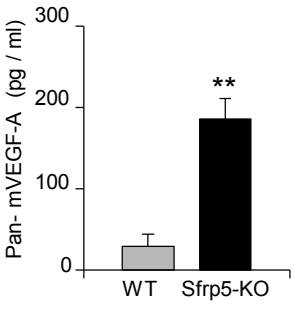

i

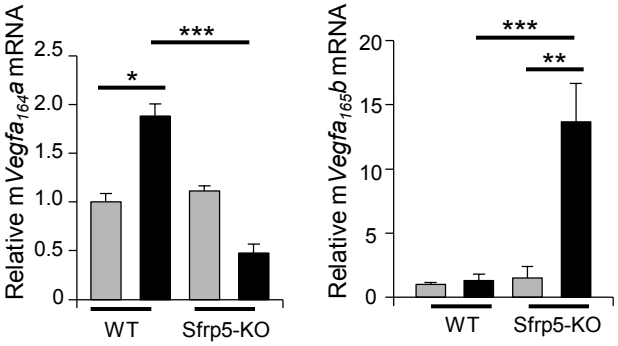

j

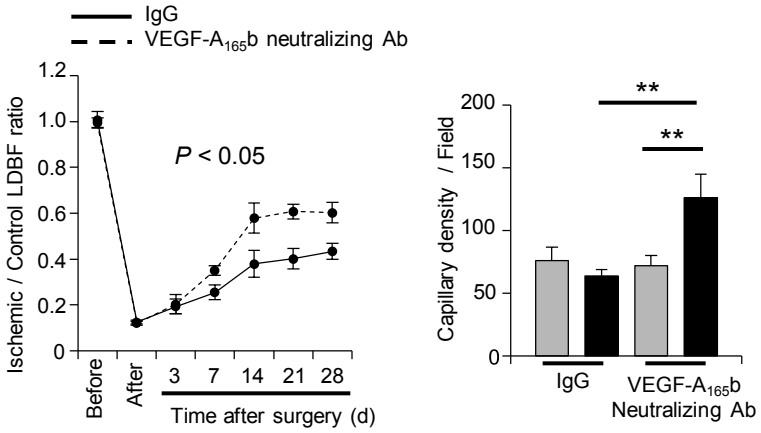

Supplementary Figure 14. VEGF-A_{165}b contributes to impaired ischemia-induced revascularization in Sfrp5-KO mice. a, Quantitative laser Doppler blood flow analysis of the ischemic/non-ischemic LDBF ratio in wild-type or Sfrp5-KO mice through postoperative day 28. Results are shown as the mean ± S.E. (*n* = 16/group). Repeated measures ANOVA. **b**, Quantitative analysis of capillary density by anti-CD31 antibody in non-ischemic (gray bar) and ischemic (black bar) muscle of wild-type or Sfrp5-KO mice on postoperative day 28. Capillary density was expressed as the number of capillaries per high power field (x200). Results are shown as the mean ± S.E. (*n* = 5/group). ANOVA with post-hoc Tukey HSD. **c**, Expression of *Wnt* family members was measured by qRT-PCR in the non-ischemic and ischemic gastrocnemius muscle of wild-type and Sfrp5-KO mice at 3 days after surgery. **d**, Wnt-5a protein expression was determined by western blot analysis in the non-ischemic (gray bar) and ischemic (black bar) gastrocnemius muscle at 3 days after surgery. Representative blots are shown from three independent experiments. Relative Wnt-5a protein was quantified using ImageJ. Immunoblots were normalized to tubulin signal. Results are shown as the mean ± S.E. (*n* = 5/group). ANOVA with post-hoc Tukey HSD. **e**, Representative pictures of immunostaining for Wnt-5a (green) and Mac2 (red) in the gastrocnemius muscle from non- (top panel) or ischemic (bottom panel) limbs. Representative images of one of five individual wild-type or Sfrp5-KO mice are shown. Scale bars are 100μm. **f**, Mac2 protein levels was determined by western blot analysis in the non-ischemic (gray bar) and ischemic (black bar) gastrocnemius muscle at 3 days after surgery in wild-type or Sfrp5-KO mice. Relative Mac2 protein was quantified using ImageJ. Immunoblots were normalized to tubulin signal. Results are shown as the mean ± S.E. (*n* = 5/group). ANOVA with post-hoc Dunnett. **g**, Total mVEGF-A, mVEGF-A_{164}a and mVEGF-A_{165}b protein expression were determined by western blot analysis in the non-ischemic (gray bar) and ischemic (black bar) muscle at 7 days after surgery. (Left) Representative blots are shown from one of three independent experiments. Relative levels of total mVEGF-A, mVEGF-A_{164}a and mVEGF-A_{165}b were quantified using ImageJ. Immunoblots were normalized to tubulin signal. Results are shown as the mean ± S.E. (*n* = 5/group). ANOVA with post-hoc Dunnett. **h**, Circulating levels of total mVEGF-A was measured by ELISA in wild-type and Sfrp5-KO mice at 7 days after surgery. (n = 5/group) Student's t-test. **i**, Expression of m*Vegfa*$_{164}$*a* and m*Vegfa*$_{165}$*b* mRNA was measured by qRT-PCR in the non-ischemic (gray bar) and ischemic (black bar) gastrocnemius muscle at 7 days after surgery. Results are shown as the mean ± S.E. (n = 5/group). ANOVA with post-hoc Tukey HSD. **j**, Sfrp5-KO mice received intraperitoneal control non-specific mouse IgG or anti-VEGF-A_{165}b neutralizing antibody (100 μg) on 0, 3 and 7 days after surgery. Quantitative analysis of the ischemic/non-ischemic laser Doppler blood flow ratio in Sfrp5-KO mice treated with anti-VEGF-A_{165}b monoclonal antibody or control mouse IgG through postoperative day 28. Results are shown as the mean ± S.E. (*n* = 8/group). Repeated measures ANOVA. Quantitative analysis of capillary density by anti-CD31 antibody staining of histological sections from Sfrp5-KO mice treated with anti-VEGF-A_{165}b monoclonal antibody or control mouse IgG on postoperative day 28. Capillary density was expressed as the number of capillaries per high power field (x200). Results are shown as the mean ± S.E. (*n* = 5) in the non-ischemic (gray bar) and ischemic (black bar) muscle. ANOVA with post-hoc Tukey HSD. **P* < 0.05, ***P* < 0.01, ****P* < 0.001.

Supplementary Figure 15.

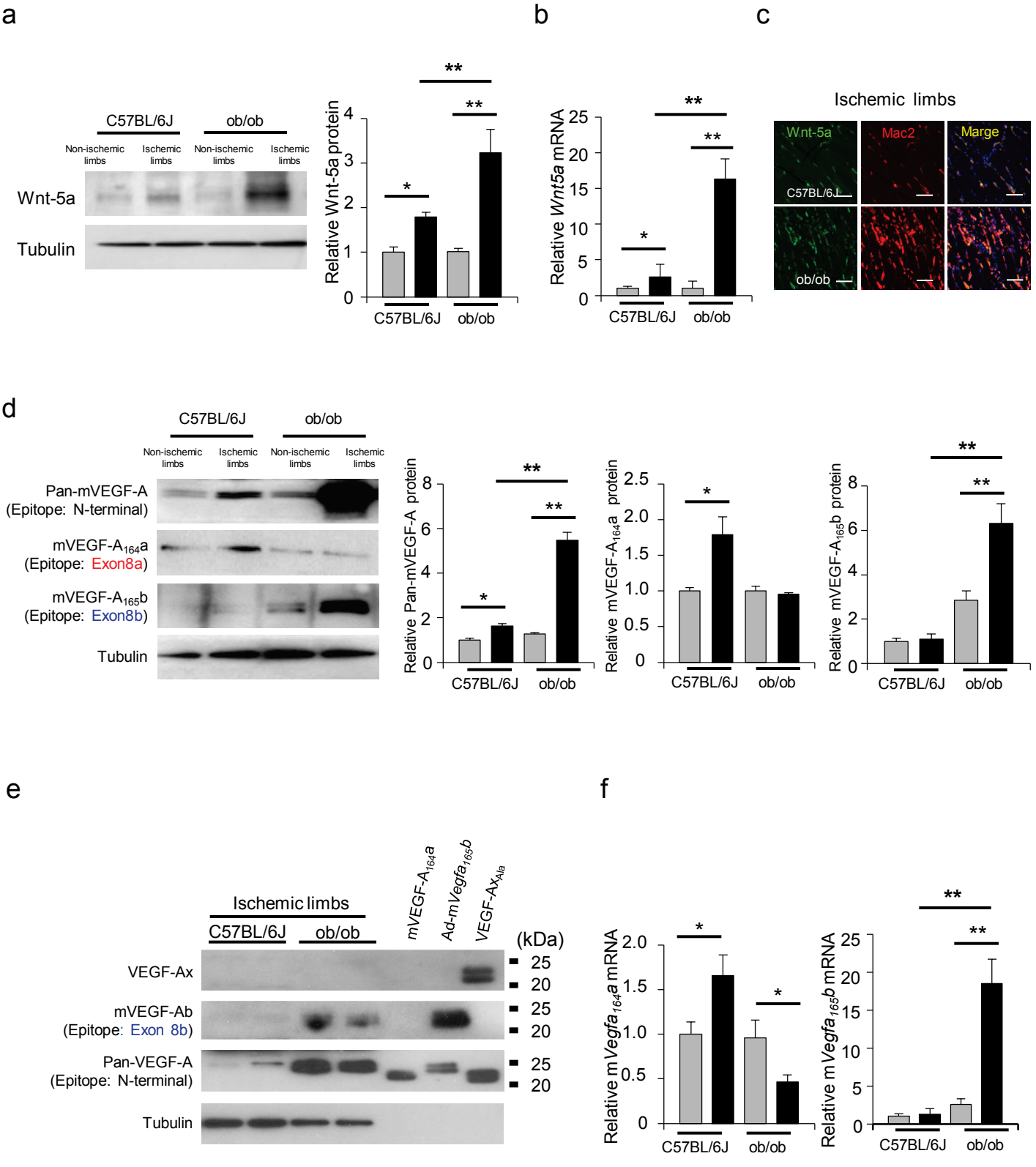

Supplementary Figure 15.

g

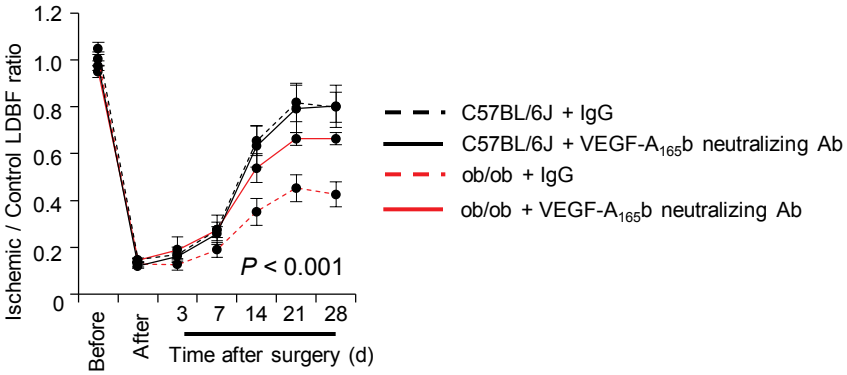

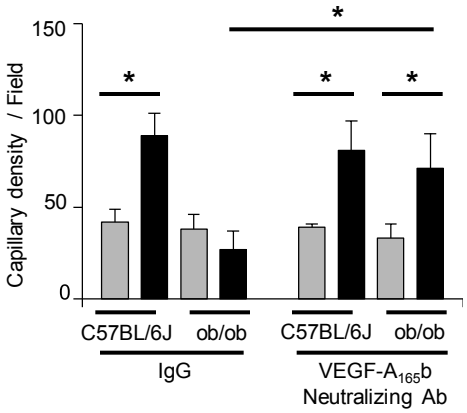

Supplementary Figure 15. VEGF-A_{165}b contributes to impaired revascularization in genetically obese (ob/ob) mice. a, Wnt-5a protein levels were determined by western blot analysis in the non-ischemic (gray bar) and ischemic (black bar) muscle 3 days after surgery. Representative blots are shown from three independent experiments. Relative Wnt-5a levels were quantified using ImageJ. Immunoblots were normalized to tubulin signal. Results are shown as the mean ± S.E. (*n* = 5/group). ANOVA with post-hoc Tukey HSD. **b**, *Wnt5a* mRNA expression was also quantified by qRT-PCR in the non-ischemic (gray bar) and ischemic (black bar) muscle at 3 days after surgery in these experimental groups. Results are shown as the mean ± S.E. (*n* = 5/group). ANOVA with post-hoc Dunnett's test. **c**, Representative images of immunostaining histological sections from gastrocnemius muscle for Wnt-5a and Mac2 in the ischemic limbs from C57BL/6J or ob/ob mice. Analysis was performed at 3 days after surgery. Scale bars are 100 μm. **d**, Total mVEGF-A, mVEGF-A_{164}a and mVEGF-A_{165}b protein levels were determined by western blot analysis in the non-ischemic (gray bar) and ischemic (black bar) muscle at 7 days after surgery. Representative blots from three independent experiments are shown. Relative levels of total mVEGF-A, mVEGF-A_{164}a and mVEGF-A_{165}b were quantified using ImageJ. Immunoblots were normalized to tubulin signal. Results are shown as the mean ± S.E. (*n* = 5/group). ANOVA with post-hoc Dunnett's test). **e**, Analysis of VEGF-Ax and VEGF-A_{165}b expression in ischemic muscle from ob/ob and control mice. **f**, Expression of m*Vegfa*$_{164}$*a* and m*Vegfa*$_{165}$*b* mRNA were measured by qRT-PCR in the non- (gray bars) and ischemic (black bars) muscle at 7 days after surgery in the different experimental groups of mice. (n = 5/group). ANOVA with post-hoc Dunnett's test. **g**, C57BL/6J or ob/ob mice in the same background received intraperitoneal anti-VEGF-A_{165}b neutralizing monoclonal antibody (100 μg) or non-specific mouse IgG on 0, 3 and 7 days after surgery. Quantitative analysis of the ischemic/non-ischemic laser Doppler blood flow ratio in the different experimental groups of mice are shown through postoperative day 28. Results are presented as the mean ± S.E. (*n* = 10). Repeated measures ANOVA. Post-hoc Tukey HSD ob/ob + IgG vs. ob/ob + anti-VEGF-A165b neutralizing antibody P = 0.04, vs C57BL/6J + IgG P = 0.001. Quantitative analysis of capillary density by anti-CD31 antibody in ob/ob versus wild-type mice treated with anti-VEGF-A_{165}b monoclonal antibody or control mouse IgG on postoperative day 28. Capillary density is expressed as the number of capillaries per high power field (x200) and capillaries per field. Results are shown as the mean ± S.E. (*n* = 5/group). ANOVA with post-hoc Tukey HSD. **P* < 0.05, ***P* < 0.01

Supplementary Figure 16.

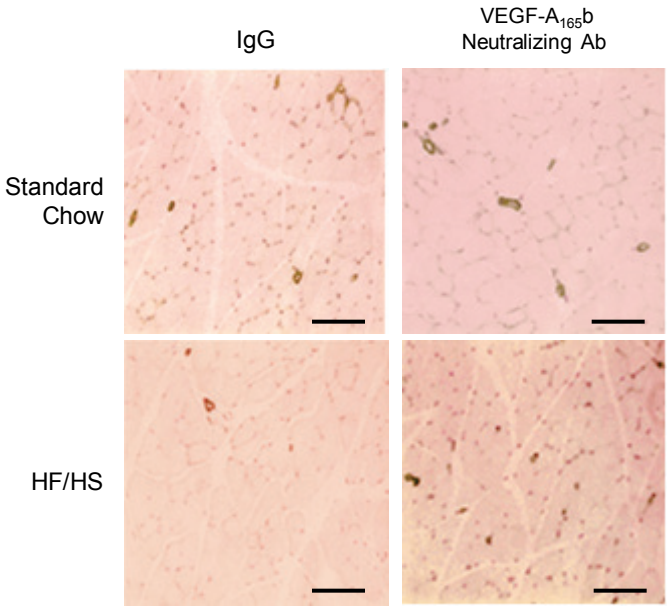

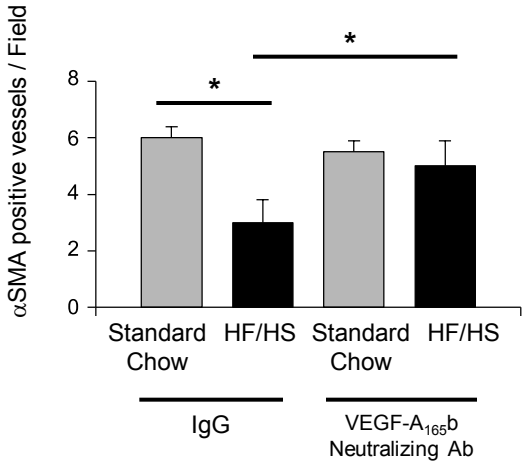

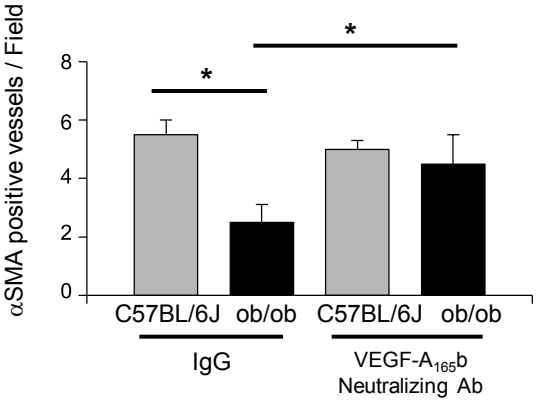

Supplementary Fig. 16. Modulation of arteriogenesis by obesity and VEGF-A_{165}b neutralization. Top: representative photomicrographs of aSMA-positive arterioles in the gastrocnemius muscle of ischemic limbs of standard chow and HF/HS mice treated with the IgG or VEGF-A_{165}b neutralizing antibody (five individual mice from each group). Scale bars are 100 μm. Middle: quantitative analysis of arteriole density in standard chow or HF/HS mice was performed at postoperative day 28. Bottom: Quantitative analysis of arteriole density in ischemic limbs of C57BL/6J or ob/ob mice, performed on postoperative day 28, that were treated with IgG or the VEGF-A_{165}b neutralizing antibody. Five mice were examined for each experimental group. For quantitative analysis, five randomly selected microscopic fields from four different sections per mouse were randomly selected. Data are presented as number per high power field; 200X magnification. ANOVA post-hoc testing with Dunnett's test. *$P < 0.05$.

Supplementary Table 1: Clinical Characteristics

	No PAD (n = 25)	PAD (n = 25)
Age, years	58 ± 6	60 ± 6
Female sex, %	44	44
Black race, %	32	48
Diabetes mellitus, %	0	36*
Hypertension, %	8	84*
Hypercholesterolemia, %	0	68*
Smoking ever, %	16	84*
Family history of CAD, %	20	44
Body mass index, kg/m^2	27.1 ± 5.9	30.5 ± 7.1
Total cholesterol, mg/dl	216 ± 40	176 ± 50*
LDL cholesterol, mg/dl	139 ± 34	105 ± 36*
HDL cholesterol, mg/dl	54 ± 14	42 ± 13*
Triglycerides, mg/dl	113 ± 60	157 ± 114
Fasting glucose, mg/dl	86 ± 13	130 ± 46*
Systolic blood pressure, mmHg	121 ± 12	143 ± 18*
Diastolic blood pressure, mmHg	72 ± 11	74 ± 11
Ankle-brachial index	1.13 ± 0.07	0.69 ± 0.25*

Data expressed as Mean ± SD
*P < 0.05
PAD, peripheral artery disease; CAD, coronary artery disease

Supplementary Table 2. Primers list for qRT-PCR.

Gene Name	Forward	Reverse
h*GAPDH*	5'-AATCCCATCACCATCTTCCA-3'	5'-TGGACTCCACGACGTACTCA-3'
h*VEGFA$_{165}$a*	5'-GAGCAAGACAAGAAAATCCC-3'	5'-CCTCGGCTTGTCACATCTG-3'
h*VEGFA$_{165}$b*	5'-GAGCAAGACAAGAAAATCCC-3'	5'-GTGAGAGATCTGCAAGTACG-3'
h*WNT5A*	5'-CAACTGGCAGGACTTTCTCA-3'	5'-TTCTTTGATGCCTGTCTTCG-3'
h*sFLT1*	5'-ATCACTAAGGAGCACTCCATCA-3'	5'-TGTTGCAGTGCTCACCTCTGA-3'
m*Gapdh*	5'-TCACCACCATGGAGAAGGC-3'	5'-GCTAAGCAGTTGGTGGTGCA-3'
m*Vegfa$_{164}$a*	5'-CAGAAAATCACTGTGAGCCTTGTT-3'	5'-CTTGGCTTGTCACATCTGCAA-3'
m*Vegfa$_{165}$b*	5'-CAGAAAATCACTGTGAGCCTTGTT-3'	5'-CTTTCCGGTGAGAGGTCTGC-3'
m*sFlt1*	5'-ATGCGTGCAGAGCCAGGAAC-3'	5'-GGTACAATCATTCCTCCTGC-3'
m*Wnt1*	5'-ATAGCCTCCTCCACGAACCT-3'	5'-GGAATTGCCATTTGCACTCT-3'
m*Wnt2*	5'-GGTCAGCTCTTCATGGTGGT-3'	5'-ATCTCTGTCCAGGGTGTTGC-3'
m*Wnt2b*	5'-TCAACGCTACCCAGACATCA-3'	5'-ACCACTCCTGCTGACGAGAT-3'
m*Wnt3*	5'-AGGAGTGCCAGCATCAGTTC-3'	5'-ACTTCCAGCCTTCTCCAGGT-3'
m*Wnt3a*	5'-CTGGCAGCTGTGAAGTGAAG-3',	5'-TGGGTGAGGCCTCGTAGTAG-3'
m*Wnt4*	5'-CTGGAGAAGTGTGGCTGTGA-3',	5'-CAGCCTCGTTGTTGTGAAGA-3'
m*Wnt5a*	5'-CAAATAGGCAGCCGAGAGAC-3	5'-CTCTAGCGTCCACGAACTCC-3'
m*Wnt5b*	5'-CTGCTTGCGTAATGAGACCA-3'	5'-AAAGCAACACCAGTGGAACC-3'
m*Wnt6*	5'-TCAGTTCCAGTTCCGTTTCC-3'	5'-CATGGAACAGGCTTGAGTGA-3'
m*Wnt7a*	5'-GGTGCGAGCATCATCTGTAA-3'	5'-TCCTTCCCGAAGACAGTACG-3'
m*Wnt7b*	5'-AAGCCTATGGAGACGGACCT-3'	5'-TTGGTGTACTGGTGCGTGTT-3'
m*Wnt8a*	5'-AGCACAGAGGCTGAGCTGAT-3'	5'-TCTGCTCTCCTCTCCTCCAC-3'
m*Wnt8b*	5'-GTGGACTTCGAAGCGCTAAC-3'	5'-CTGCTTGGAAATTGCCTCTC-3'
m*Wnt9a*	5'-TGCTTTCCTCTACGCCATCT-3'	5'-CCTTGACAAACTTGCTGCTG-3'
m*Wnt9b*	5'-TGGAGCGCTGTACTTGTGAC-3'	5'-GCACTTGCAGGTTGTTCTCA-3'
m*Wnt10a*	5'-CATGAGTGCCAGCATCAGTT-3'	5'-ACCGCAAGCCTTCAGTTTAC-3'
m*Wnt10b*	5'-GGAAGGGTAGTGGTGAGCAA-3',	5'-CTCTCCGAAGTCCATGTCGT-3'
m*Wnt11*	5'-CAGGATCCCAAGCCAATAAA-3'	5'-GTAGCGGGTCTTGAGGTCAG-3'
m*Wnt16*	5'-GAGCTGTGCAAGAGGAAACC-3'	5'-TGAATGCTGTCTCCTTGGTG-3'